AMD-Vol. 149, Web Handling
ASME 1992

A NONLINEAR WOUND ROLL STRESS MODEL ACCOUNTING FOR WIDTHWISE WEB THICKNESS NONUNIFORMITIES

Kevin A. Cole and Zig Hakiel
Department of Manufacturing Research and Engineering
Coating Technologies Division
Eastman Kodak Company
Rochester, New York

ABSTRACT

A model has been developed which predicts widthwise variability in wound roll radius and stresses resulting from widthwise thickness nonuniformities. This model has been verified experimentally on wound rolls of film and quantitative agreement between the predicted and measured results was found. The theoretical and experimental techniques used in its verification are described.

NOMENCLATURE

$a_s(i,j)$, $b_s(i,j)$	scaling coefficients in tension/deflection relationship, where i designates lap number and j designates widthwise segment
E	Young's modulus of the web in the length direction
h(j)	widthwise thickness distribution
m	number of axial segments
$r_d(i,j)$	deflected roll outer radius prior to "winding" of next lap
$r_o(i)$	nominal relaxation radius
t(i)	total winding tension
$t_a(i,j)$	partitioned winding tension, $\sigma_a(i,j)w(j)h(j)$
$t_{ao}(i,j)$	initial partitioned winding tension
U'(i,j)	incremental roll displacement due to i^{th} lap
w(j)	segment width
ε_θ	circumferential strain
$\sigma_a(i,j)$	partitioned winding tension stress
ν_w	Poisson's ratio of web (effect of length direction tension on width direction strain)

INTRODUCTION

The trend within industry today is to develop manufacturing processes which are capable of producing products which are of the

highest quality possible at the lowest cost. To achieve this goal, it is critical that the impact of each process parameter on the quality metric be fully understood. One means to achieve this is to develop accurate analytical math models which can be used to quickly study the effects of these parameters.

Wound roll technology is one such process that can benefit greatly from this approach. Several classes of problems exist in this technology for which robust math models have not been available. One such class of problems involve widthwise effects within winding and wound rolls. Included in this class of problems are what are commonly called hardstreaks. These are areas of increased hardness (and interlayer pressure) within the roll which can be formed by lengthwise persistent widthwise variations in web thickness. Hardstreaks can give rise to a host of problems which cause degradation in the finished product. Examples include permanent distortion due to stress relaxation and layer-to-layer adhesion due to extreme values of interlayer pressure.

A great deal of literature exists on the subject of wound roll stresses. Only a few of the most pertinent works will be cited here. What would be considered by most in the field to be the start of modern in-roll stress modeling was performed by Altmann (1968). His model considers the center winding process as a sequence of individual hoops added one at a time to the roll. The web is treated as a linear orthotropic material and only radial effects are considered. Despite the severe limitation of the model due to the material assumption, it proved useful early on in explaining qualitatively many observed roll phenomena. Subsequently, a nonlinear model was developed by Hakiel (1987) which incorporates the load-dependent radial stiffness (stack modulus) using a finite difference solution technique. This model is significant in that it is of practical use for simulation and yields results which agree quite well with experiment. Again, however, only radial effects are considered.

An attempt at incorporating width effects into a wound roll stress model was made by Hakiel (1991) and represents a simple extension to his previous work (1987). The model predicts widthwise variations in the outside roll radius (roll profile) and winding tension based on widthwise thickness variations of the web, mechanical properties of the web, and the nominal value of winding tension. The model then employs the in-roll stress algorithm described by Hakiel (1987) to compute the in-roll stresses for the various widthwise segments of the roll. The model was shown to yield results which agree favorably with experiment for certain cases; however, the lack of coupling between the outerlap analysis and the in-roll displacements prevents its application for more general cases where web compressibility is important. Most recently, a model was developed by Kedl (1991) which again considers width effects. An effort to couple in-roll displacements with the outer lap analysis was made. For this purpose, a special model based upon stacking thick walled cylinders with orthotropic properties was used. This implementation, while an improvement over Hakiel (1991), nevertheless neglects the dependence of stack modulus on load when calculating in-roll displacements.

The model presented herein is similar to Kedl (1991) in that coupling between the outer lap analysis and the in-roll displacements is accounted for. The major difference is that the coupling occurs at each lap in the program while the roll is winding. This provides the means to retain the effect of the load-dependent stack modulus on in-roll displacements.

The model is used to simulate the winding of .254-meter-wide rolls of polyethylene terephathalate (PET) film for which experimental data are available as discussed by Hakiel (1991). The

new model is shown to yield answers which are in excellent agreement to those results.

THEORETICAL MODEL

Overview

The objective of this model is to predict the widthwise variations in outside roll radius, winding tension, interlayer pressure, and in-roll tension in a roll wound of a web with lengthwise-persistent widthwise thickness variations. For this purpose, the roll is partitioned in the widthwise direction into a discrete number of segments. Within each segment, the process parameters as well as the stresses and displacements are width independent.

An outerlap analysis based on equilibrium considerations is used to partition the winding tension for a particular lap. The widthwise distribution of the outside roll radius, the total winding tension in the lap, and the radial displacements in each segment due to the lap are used in the calculations. The stresses and displacements within the segments are calculated using the algorithm described by Hakiel (1987).

Derivation

Consider a winding roll with a widthwise-varying radius or roll profile as shown in Figure 1. Prior to the addition of the next lap, say the i^{th}, the roll will have a widthwise-varying radius, $r_d(i,j)$, where j indicates axial segment. Now, the next lap under total tension, t(i), is added to the roll. This lap may or may not make full contact with the roll. In segments where contact is made, the lap being wound will cause radial displacement while in segments where there is no contact, no tension will exist in the lap. The lap in the segments where no contact (or gapping) occurs will be suspended as a straight cylindrical surface above the roll. Figure 2 illustrates this condition. The radius to the centerline of the unstretched lap of web is given by $r_o(i)$ and is referred to as the relaxation radius.

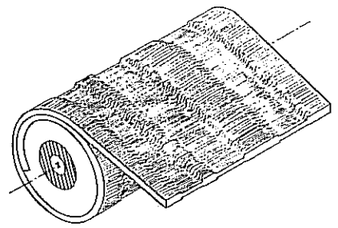

Figure 1 - Winding Geometry, Imperfect Roll

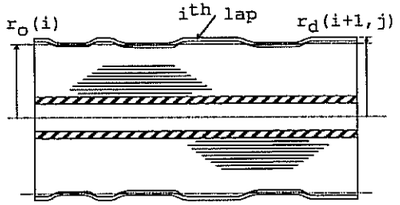

Figure 2 - Winding Geometry Cross Section - Imperfect Roll

To proceed, the relationship between the partitioned winding tensions, $t_a(i,j)$, and the relaxation radius must be determined. For this purpose, the roll profile after addition of the i^{th} lap, $r_d(i+1,j)$ is defined for segments which do not gap as (see Figure 3)

$$r_d(i+1,j) = r_d(i,j) + U'(i,j) + h(j) \quad \text{(no gapping)} \tag{1}$$

where $U'(i,j)$ is the radial displacement of the segment due to the i^{th} lap and is defined positive radially outward. For segments which gap, the roll profile after addition of the i^{th} lap is

$$r_d(i+1,j) = r_o(i) + \frac{h(j)}{2} \quad \text{(gapping)}. \tag{2}$$

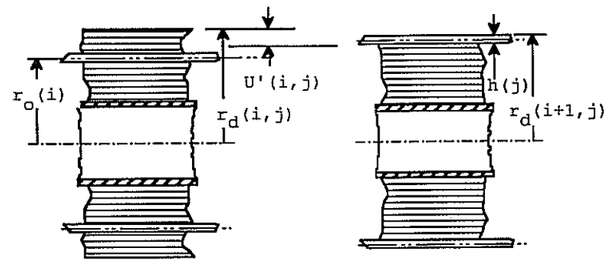

(a) before addition of ith lap (b) after addition of ith lap

Figure 3 - Outer Lap Geometry

The circumferential tensile strain in the outer lap can be expressed as

$$e_\theta = \frac{r_d(i+1,j) - \frac{h(j)}{2} - r_o(i)}{r_o(i)} \tag{3}$$

where $r_d(i+1,j)$ takes the form of either equation (1) or (2) depending on whether or not gapping occurs in the segment. The winding tension stress due to this strain can now be written (assuming no slip in the width direction) for any segment as

$$\sigma_\theta(i,j) = \frac{E}{1-\nu_w^2}\left(\frac{r_d(i+1,j) - \frac{h(j)}{2} - r_o(i)}{r_o(i)}\right). \tag{4}$$

Observation of equation (4) indicates that the partitioned winding tension stress, $\sigma_\theta(i,j)$, for each lap has to be determined recursively for three reasons. First, the relaxation radius is unknown a priori as is the contact condition of each segment (ungapped or gapped). Lastly, the radial displacement within each segment depends directly on the winding tension stress.

The last condition is addressed by recalling assumptions which are used in solving the purely radial wound roll stress problem (Hakiel, 1987). In that case, the winding of a roll is considered to be an incremental process consisting of adding successive laps onto the roll. Before each lap is added, the model assumes elastic properties based on the radial stress distribution. As each lap is added, the elastic properties do not vary and the winding tension in the lap being added is constant. Thus, the incremental process of adding a single lap is linear with respect to winding tension. Because of this linearity, the radial displacement due to the i^{th} lap

can be written as a linear function of the partitioned winding tension, $t_a(i,j)$:

$$U'(i,j) = U'_o(i,j)\,\frac{t_a(i,j)}{t_{ao}(i,j)} \tag{5}$$

where $U'_o(i,j)$ is the radial displacement of the j^{th} segment under the i^{th} lap due to an arbitrary partitioned winding tension, $t_{ao}(i,j)$. Substitution of equations (5) and (1) into (4) with the constraint that the term in parenthesis cannot go negative (implying gapping) yields

$$\sigma_\theta(i,j) = \frac{E}{1-\nu_w^2}\left(\frac{a_s(i,j) + b_s(i,j)\,t_a(i,j) - r_o(i)}{r_o(i)}\right) \tag{6}$$

where the coefficients $a_s(i,j)$ and $b_s(i,j)$ are given by

$$\begin{aligned} a_s(i,j) &= r_d(i,j) + \frac{h(j)}{2} \\ b_s(i,j) &= \frac{U'_o(i,j)}{t_{ao}(i,j)} \end{aligned} \tag{7}$$

and are independent of the partitioned winding tension. Using the relationship between winding tension stress and winding tension

$$\sigma_\theta(i,j) = \frac{t_a(i,j)}{w(j)h(j)} \tag{8}$$

equation (6) can be rewritten to yield

$$t_a(i,j) = \frac{a_s(i,j) - r_o(i)}{\frac{1-\nu_w^2}{Ew(j)h(j)}\,r_o(i) - b_s(i,j)}. \tag{9}$$

The relationship between the partitioned winding tension and the relaxation radius is established by equation (9). By summing the partitioned winding tensions across the width of the web, an expression for the total winding tension is obtained

$$t_{pred}(i) = \sum_{j=1}^{m} t_a(i,j). \tag{10}$$

This predicted value of the winding tension must equal the total winding tension for the i^{th} lap, $t(i)$, in order to satisfy equilibrium in the outer lap

$$t_{pred}(i) = t(i). \tag{11}$$

Care must be taken in the solution of equation (11) owing to the potential for gapping. To proceed, a value for the relaxation radius is selected and total predicted winding tension calculated using equation (11). A second guess is made and the process repeated. Subsequent guesses are made using the secant method until convergence is obtained to within a relative tolerance, eps

$$\text{abs}\left(\frac{t_{pred}(i) - t(i)}{t(i)}\right) \le \text{eps}. \tag{12}$$

During the iterations, partitioned tensions within segments may possibly be negative. If so, the algorithm identifies the segment with the most negative tension. The tension in that segment is set to zero (gapping) and the iteration procedure described above repeated. The process continues with one segment at a time allowed to gap until complete convergence is obtained.

Upon convergence, the segments which have gapped for the first time are identified. During addition of subsequent laps, gapped segments are not allowed to close although the program checks to verify the accuracy of the assumption.

Finally, the in-roll displacements and stresses due to the i^{th} lap are determined by scaling the results from the in-roll analysis for each segment and the roll profile updated according to either equation (1) or (2). The process continues until the roll is completely wound. The computational scheme described above is illustrated in the flowchart of Figure 4.

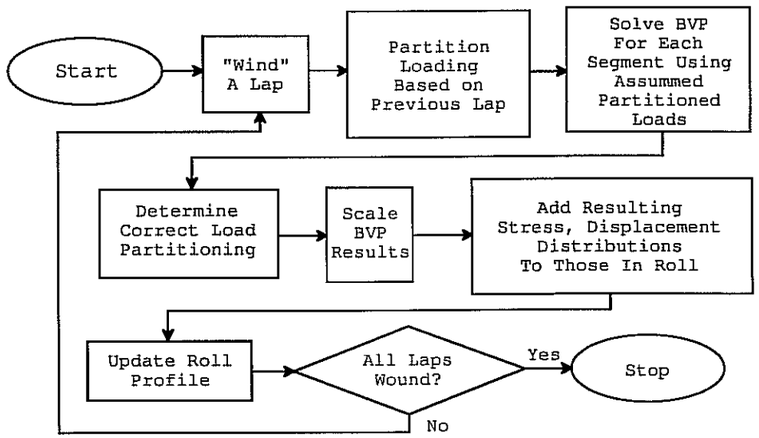

Figure 4 - Flow Chart of Width Effects Model

EXPERIMENTS

Roll Profile Measurement

Roll profile is the widthwise distribution of the outside winding roll radius. An instrument for measuring roll profile was constructed and is shown in Figure 5. It consists of a carriage mounted LVDT for sensing radius nonuniformities. This carriage traverses the roll width on two rods. A potentiometer-based displacement transducer is connected to the carriage to measure widthwise position of the LVDT. This permits the recording of roll radius variations as a function of width on an X-Y recorder. The entire carriage and rod assembly is mounted on a larger carriage which rides in the radial direction, thus permitting measurement of the roll profile to be made at various roll radii. The LVDT selected for this instrument is air loaded and generates a contact force of approximately 0.14 N. This light loading does not appear to significantly deform the surface of the roll being measured.

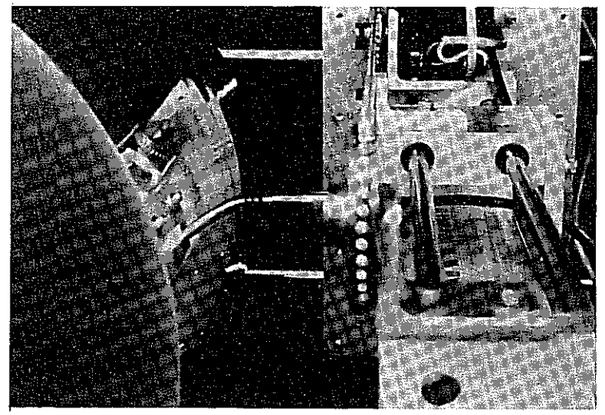

Figure 5 - Photograph of Roll Profile Measurement Instrument

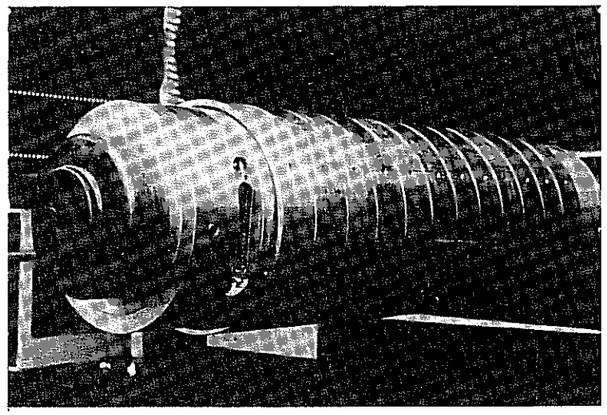

Figure 6 - Photograph of Segmented-Instrumented Core

Interlayer Pressure Measurement

In order to measure the widthwise variations of interlayer pressure, a segmented-instrumented core was constructed. This core is capable of measuring the interlayer pressure at the core in 2.54-cm widthwise segments. The core which was constructed for these experiments was a 12.7-cm diameter aluminum core consisting of twelve independent 2.54-cm wide segments. Each of the segments in

this core is instrumented with two strain gauges which measure the circumferential contraction of the segment. All of the segments are mounted on a common inner core by means of rubber "O-rings" and are pinned to the inner core with three pins. This allows the segments to contract radially, independently of each other and of the inner core. It also allows torque to be transmitted from the inner core to the segments and on to the winding roll. The inner core also houses all of the cables coming from and going to the strain gauges on the segments as well as the connector to which these cables are attached. Temperature compensation strain gauges are also mounted on one of the end plates of the inner core. A photograph of the segmented-instrumented core is shown in Figure 6.

Pressure readings are obtained with the segmented-instrumented core once the roll becomes stationary and a cable connected from the core to a signal conditioner/readout. Readings are sequentially obtained for each of the segments via a selector switch. In order to verify the predicted relationship between the strain level in the core segments and pressure on the core, a calibration fixture was built and utilized. This fixture consists of a metal vessel which slips over the core and which contains a rubber tube inside. To calibrate the core, the fixture is slipped over the core and the tube is inflated with a gas at a known pressure. The gain of the signal conditioner can then be adjusted to give readouts of pressure equal to air pressure in the rubber tube.

Verification Experiments

In the verification experiments, two 25.4-cm-wide webs of .102-mm PET were wound on the segmented-instrumented core at two levels of winding tension: 3.5 N/cm and 7.0 N/cm. The rolls were wound at the low speed of 63.5 cm per sec in order to minimize the effects of air entrainment on in-roll stresses. During the winding of each of the rolls, the winder was stopped several times with the tension maintained in the machine, so that measurements of roll profile and pressure at the core could be performed.

Once the winding experiments were completed, samples were cut from the two PET webs, so that widthwise thickness measurements could be made. Thirty equally spaced widthwise thickness traces were made for each of the webs using a contacting thickness gauge interfaced with a data acquisition system. The thirty traces were then averaged in the lengthwise direction to obtain average widthwise thickness traces for each web.

RESULTS AND DISCUSSION

The average widthwise thickness traces obtained for the two PET webs used in the verification experiments are shown in Figures 7 and 8. From the thickness data, the nominal winding tension values used in the experiments, and previously measured mechanical properties for the PET webs, the model was used to predict roll profiles and pressure distributions at the core. Inputs to the winding model are shown in Table 1.

First consider the roll profile results. Figures 9 through 12 show the measured values alongside those generated by the model. Predicted results are shown from the current model (outer lap analysis coupled to radial displacements) and from that of Hakiel (1991) (outer lap analysis uncoupled to radial displacements). From a comparison of these data, it is seen that, while qualitative agreement exists in all cases, the coupled version gives results which are in much closer agreement quantitatively to the experimental data. It is also informative to observe that the coupled results correctly indicate the lack of gapping. Inclusion of radial displacements in the analysis thus greatly improves the

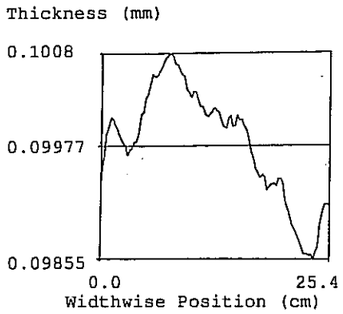

Figure 7 - Average Width Thickness Trace For Roll A

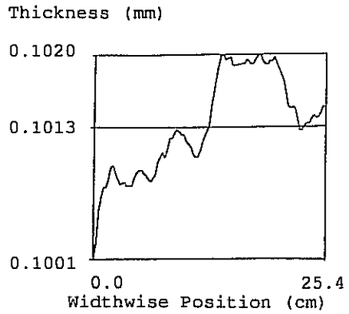

Figure 8 - Average Width Thickness Trace For Roll B

Table 1 - Model Inputs

Core Diameter	12.7 cm
Finish Roll Diameter	38.1 cm
Web Thickness	0.102 mm
Young's Modulus	4.339 GPa
Stack Modulus	Exponential Function, $C_0\left(1-e^{\frac{-pressure}{C_1}}\right)$
	C_0 = 2.4949 GPa
	C_1 = 8.6496 MPa
Poisson's ratio	0.01
Core Modulus	3.534 GPa
Winding Tension Profile	Constant Tension, 3.5 and 7.0 N/cm

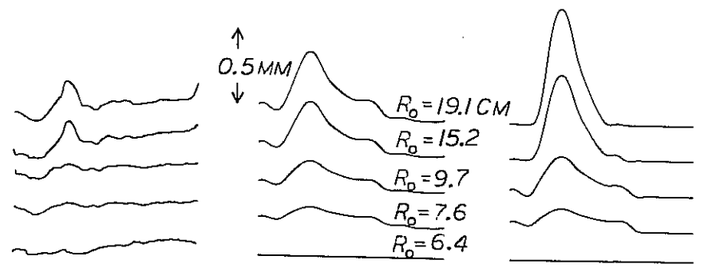

Measured Predicted (Coupled) Predicted (Uncoupled)

Figure 9 - Roll Profiles for Roll A Wound at a Tension of 3.5 N/cm

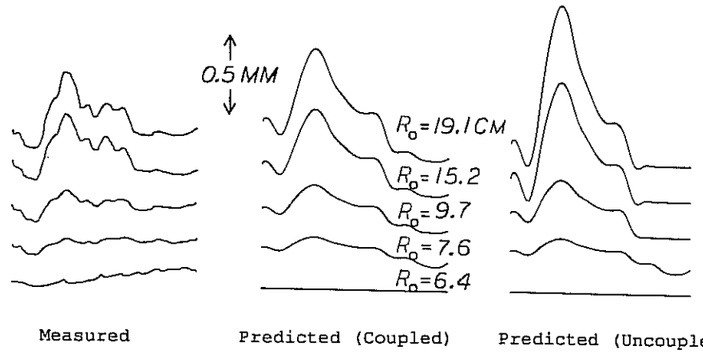

Figure 10 - Roll Profiles for Roll A Wound at a Tension of 7.0 N/cm

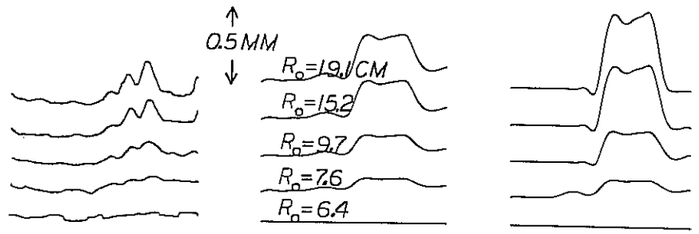

Figure 11 - Roll Profiles for Roll B Wound at a Tension of 3.5 N/cm

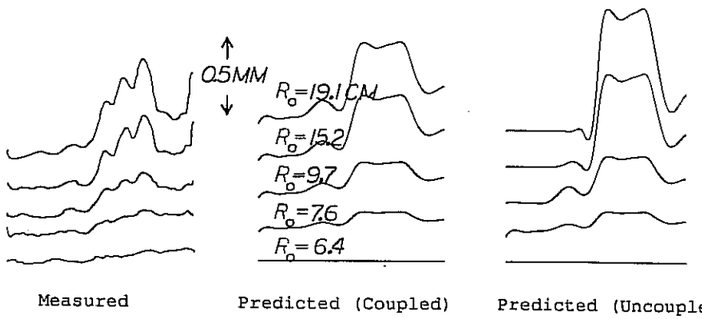

Figure 12 - Roll Profiles for Roll B Wound at a Tension of 7.0 N/cm

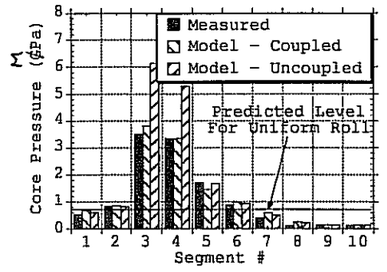

Figure 13 - Core Pressure For Roll A Wound With a Tension of 3.5 N/cm

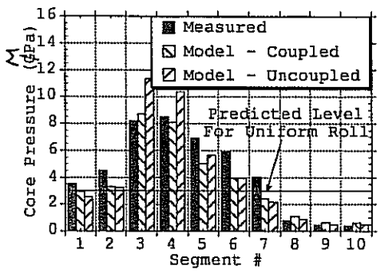

Figure 14 - Core Pressure For Roll A Wound With a Tension of 7.0 N/cm

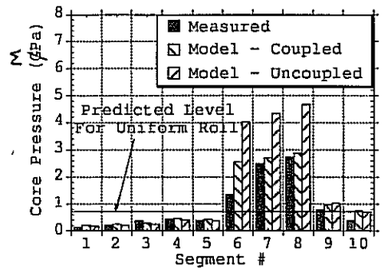

Figure 15 - Core Pressure For Roll B Wound With a Tension of 3.5 N/cm

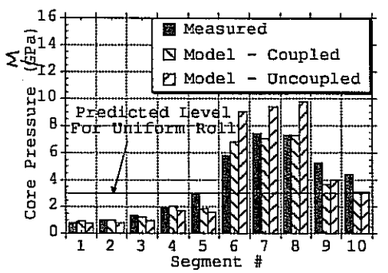

Figure 16 - Core Pressure For Roll B Wound With a Tension of 7.0 N/cm

correlation between predicted and measured roll profile results. This would suggest that the partitioning methodology of the current model which neglects bending stiffness for the web is valid. This conclusion is supported by Kedl (1991) and more recent work by Benson and D'Errico (1991).

For both of the webs used in the experiment, the measured and predicted roll profiles tend to roughly follow the shape of the average widthwise thickness distribution. In areas where thickness is high, the roll profile tends to have peaks or hardstreaks, and in areas where thickness is low, the roll profile tends to have low spots or valleys. This is due to the lengthwise persistence of the widthwise thickness nonuniformity. If there are many such high spots in the average thickness profile, the winding tension becomes distributed over a number of hardstreaks and none of them is very severe. However, it there are only a few areas in the widthwise thickness distribution which are significantly higher than the rest of the web, severe hardstreaks will develop in those areas.

Interlayer pressures at the cores of the fully wound rolls are shown in Figures 13 through 16. The model results were generated for 20 equally spaced segments with successive pairs averaged to

yield the 10 outputs shown in the figures. Results are again shown from both the coupled and uncoupled version of the model as well as from the experiments. The core pressure values which would exist in the rolls of PET if the thickness of the web were perfectly uniform were also calculated with the model for comparison and are included in the figures.

Observation of the plots indicates that the present model yields results which agree quite well quantitatively with the experimental data. This agreement results from the high pressure segments exhibiting a reduction in pressure as compared to the uncoupled model. Low pressure segments, on the other hand, exhibit the opposite behavior. This change is the direct result of including the effect of in-roll displacements which tend to reduce the variations in partitioned winding tension from the variations which exist when excluding the in-roll displacements in the model.

SUMMARY AND CONCLUSIONS

An improved model for computing widthwise variations in roll radius and in-roll stresses caused by widthwise web thickness variations was described. A novel method was presented for incorporating the coupling between in-roll displacements and widthwise tension partitioning in the outer lap. The model was verified quantitatively on two rolls of PET film with the use of a roll profile measurement instrument and a segmented-instrumented core. Hardstreak severity was found to be dependent on the winding tension level and the number and amplitude of widthwise thickness variations in the web. It was found that for the rolls used in the experiments that the actual maximum interlayer pressure in the rolls was significantly higher than the pressure which would have been predicted for a uniform roll.

REFERENCES

Altmann, H. C., 1968,"Formulas for Computing the Stresses in Center-Wound Rolls," *Tappi Journal*, Vol. 51, No. 4, pp. 176-179.

Benson, R. C., and D'Errico, J. R., 1991,"The Deflection of an Elastic Web Wrapped Around a Surface of Revolution," *Mechanics of Structures and Machines*, Vol. 19, No. 4, pp. 457-476.

Hakiel, Z., 1987,"Nonlinear Model for Wound Roll Stresses", *Tappi Journal*, Vol. 70, No. 5, pp. 113-117.

Hakiel, Z., 1991,"On the Effect of Width Direction Thickness Variations in Wound Rolls," *Proceedings, First International Conference on Web Handling*, Oklahoma State University, to be published.

Kedl, D. M., 1991,"Using a Two Dimensional Winding Model to Predict Wound Roll Stresses that Occur Due to Circumferential Steps in Core Diameter or to Cross-Web Caliper Variation," *Proceedings, First International Conference on Web Handling*, Oklahoma State University, to be published.